on {100}, {111}, and {110} planes in the range between 11 and 30 Å were taken into account and an experimentally observed line was found to coincide with the calculated energy except for those denoted on Fig. 1 by B_n.[9] The B_n lines and bands form an abosrption spectrum which is a "mirror" image of the luminescence spectrum of the crystals; these lines are excluded from my interpretation because they belong to center of another type.

A definitive explanation of the experimental observations is not possible at this time. However, the following hypothesis is advanced. The second term in Eq. (1) can be interpreted as the binding energy of an exciton if it is assumed that the parameter a is equivalent to a Bohr radius. Let us assume that excitons can be bound to dislocation loops. The dimensions of such loops should change by increments of interatomic spacing in the lattice. If it is assumed that the binding energy of an exciton to a dislocation loop depends on the dimensions of the loop, one would expect the energy of the exciton–dislocation-loop complex to change incrementally in a similar way. While it may be surprising to find a close correlation between dimensions of dislocation loops and the Bohr radius of the bound excitons, the experimental results certainly indicate that this model could explain the observed fine structure.

Another possible explanation begins with the observation that dislocation loops produce dangling bonds and strain in their vicinity. Such dangling bonds may act as donor and acceptor states as in glasses and amorphous semiconductors.[10] These defects may produce shallow donor and acceptor states whose ionization energies may be functions of dislocation-loop dimensions. Transitions between donor-acceptor states of this kind could then give rise to the observed fine structure.

The author is deeply indebted to Professor J. J. Loferski for his many helpful discussions.

[1]R. E. Nahory and H. Y. Fan, Phys. Rev. 156, 825 (1967).

[2]E. Giaro, Phys. Status Solidi (a) 14, K117 (1972).

[3]W. Wardzyński and I. Turska, in Proceedings of the Polish Conference on Luminescence, Toruń, Poland, 1972 (unpublished).

[4]W. Wardzyński, J. Piotrowski, K. Pataj, and I. Turska, J. Lumin. 14, 295 (1976).

[5]Z. Liliental and H. Bartsch, Phys. Status Solidi (a) 34, K5 (1976).

[6]The author is grateful to Z. Liliental for permission to use this information prior to publication.

[7]E_g was found from the $n = 1$ and $n = 2$ free-exciton peaks observed in reflection.

[8]*Physics and Chemistry of II-VI Compounds*, edited by M. Aven and J. S. Prenner (North-Holland, Amsterdam, 1967), pp. 127, 566.

[9]If one takes into account plane types other than {100}, {110}, and {111} which are possible sites of interstitial-type dislocation loops with Burgers vectors of the $a/2$ [110] type, one finds only three Zn-Zn separations different from those associated with the three principal planes. One of these separations (a = 16.7313 Å) results in a line at 18 928.37 cm^{-1}. There is a line at 18 929.5 cm^{-1} between lines No. 7 and No. 8 of Fig. 1 which may belong to this a value. The other two Zn-Zn separations would result in lines so close to No. 14 and No. 15, respectively, that they would not be resolvable with our instrumentation.

[10]R. A. Street and N. F. Mott, Phys. Rev. Lett. 35, 1293 (1975).

Exchange Splitting in Nickel

Eberhard Dietz, Ulrich Gerhardt, and Christa J. Maetz
Physikalisches Institut der Universität Frankfurt, D-6000 Frankfurt am Main, Germany
(Received 2 November 1977)

We determine the exchange splitting in ferromagnetic Ni by means of angle-resolved photoemission from a (111) surface. The optical selection rules arising from use of the $(1\bar{1}0)$ mirror plane of detection are used to identify the contributions from the majority- and minority-spin sub-bands. The splitting at the top of the d bands turns out to be about 0.5 eV at the point $(0.14, -0.43, -0.43)2\pi/a$, in good agreement with a recent self-consistent band-structure calculation by Wang and Callaway based on the exchange potential of von Barth and Hedin.

The self-consistent calculation of the energy bands in ferromagnetic Ni by Wang and Callaway[1] gives very good agreement with the measured magneton number. It also reproduces most of the observed Fermi-surface data.[1] However, there is no generally accepted experimental value for

the exchange splitting Δ_x implied by this calculation, although several groups have tried to determine it by various methods.[2-6] We present an unambiguous spectroscopic determination of Δ_x using angle-resolved photoemission from a Ni(111) surface at photon energies $\hbar\omega = 10.2$ and 16.8 eV. In contrast to similar attempts,[5,6] we use optical selection rules to identify specific components of the 3*d* sub-bands. This method is based on the golden-rule formulation of the volume photoemission process; it was first proposed by Kane[7] and used recently to identify various individual transitions from the 3*d* states of Cu.[8]

The experimental procedure is described more fully elsewhere.[8,9] It uses plane-polarized light at normal incidence to the electropolished (111) surface, cleaned by argon-ion bombardment and annealing. The plane of detection is the mirror plane $(1\bar{1}0)$ of the crystal. The results given in Figs. 1(a) and 1(b) are obtained for photon energies $\hbar\omega = 16.8$ and 10.2 eV, respectively, with the plane of polarization perpendicular to $(1\bar{1}0)$ at an oxygen partial pressure below 10^{-10} Torr. The positive and negative sign of the polar emission angle ϑ refers to $\vec{\kappa}$ parallel to $[\bar{1}\bar{1}2]$ and $[11\bar{2}]$, respectively, where $\vec{\kappa}$ is the component of the vacuum wave vector parallel to the (111) surface of the sample.

The golden-rule formulation for the unscattered photoelectrons implies perfect periodicity in the volume and along the surface of the crystal, i.e., conservation of $\vec{k}$ in the absorption process and conservation of its component $\vec{k}_t$ parallel to the (111) surface in the emission process. The unscattered electrons reaching the detector thus originate from Bloch states $|n, \vec{k}\rangle$ with $\vec{k}$ parallel to the $(1\bar{1}0)$ mirror plane. The energy conservation during the emission requires the kinetic energy of the photoelectron in vacuum to be given by $E = E_n(\vec{k}) - \Phi$, with Φ being the work function. This equation defines the light lines of constant final energies in the $(1\bar{1}0)$ plane shown in Fig. 1. Their energy is referenced to the initial states $|m, \vec{k}\rangle$ from which the electrons have been excited by the particular photon energy, with $E_n(\vec{k}) = 0$ corresponding to an initial state at the Fermi energy E_F. They are generated by adjusting the parameters of the combined interpolation scheme[10] to the eigenvalues calculated self-consistently by Wang and Callaway[1] using the exchange-correlation potential of von Barth and Hedin (vBH).[11] The light solid lines correspond to the majority-spin sub-bands, the light dash-dotted lines to the minority-spin states. For fixed ϑ, the momentum conservation in the emission $(\vec{k}_t = \vec{\kappa})$ restricts the contribution of the final states to points on these lines, thus generating the lines of $\vec{k}_t$ conservation shown dashed in Fig. 1. Here, the angular resolution of $\pm 7°$ is incorporated. Finally, the energy conservation in the excitation process given by $\hbar\omega = E_n(\vec{k}) - E_m(\vec{k}) = E_{nm}(\vec{k})$ defines the heavy solid and dash-dotted optical lines in Fig. 1, corresponding to transitions between majority- and minority-spin states, respectively. For the sake of clarity, these lines are shown only in the $\vartheta = \pm 30°$ and $\pm 60°$ regions sampled by the four detectors and only for the occupied initial states.

According to the golden-rule expression, the number of unscattered photoelectron is given by $N(\omega, E, \vec{\kappa})\Delta\omega\,\Delta E\,\Delta\vec{\kappa}$ with

$$N(\omega, E, \vec{\kappa}) \propto \sum_{m,n} \int_{\text{B.Z.}} d^3k\, |\langle n|\vec{A}^0 \cdot \vec{p}\,|m\rangle|^2 \times \delta(E_{nm}(\vec{k}) - \hbar\omega)\,\delta(E_n(\vec{k}) - \Phi - E)\,\delta(\vec{k}_t - \vec{\kappa})\,P f(E_m)[1 - f(E_n)]. \quad (1)$$

The three δ functions describe the energy and momentum conservation discussed above; they are responsible for the optical lines, the lines of constant final energy, and the lines of $\vec{k}_t$ conservation shown in Fig. 1. P is the escape probability and f the Fermi-Dirac function. The dipole matrix element in the integrand gives rise to the optical selection rules[7] which were used already to identify the various components of the Cu *d* band.[8] The final and initial states contained in it must have a definite parity with respect to the mirror reflection at (110). The electron at the detector corresponds to a plane wave with even parity, and since the ideal surface does not change the parity of the wave function, the electrons must originate from even-parity final states $|n\rangle$.[12] For the plane of polarization perpendicular to $(1\bar{1}0)$ as used in this experiment, the dipole operator has odd parity. The matrix element is thus nonzero only for the two odd-parity initial states in the *d* band,[8] and only the two optical lines corresponding to them are shown in Fig. 1. The higher energy component of these two states corresponds to the top of the *d* band, it is most important for our analysis since it will be above or below E_F

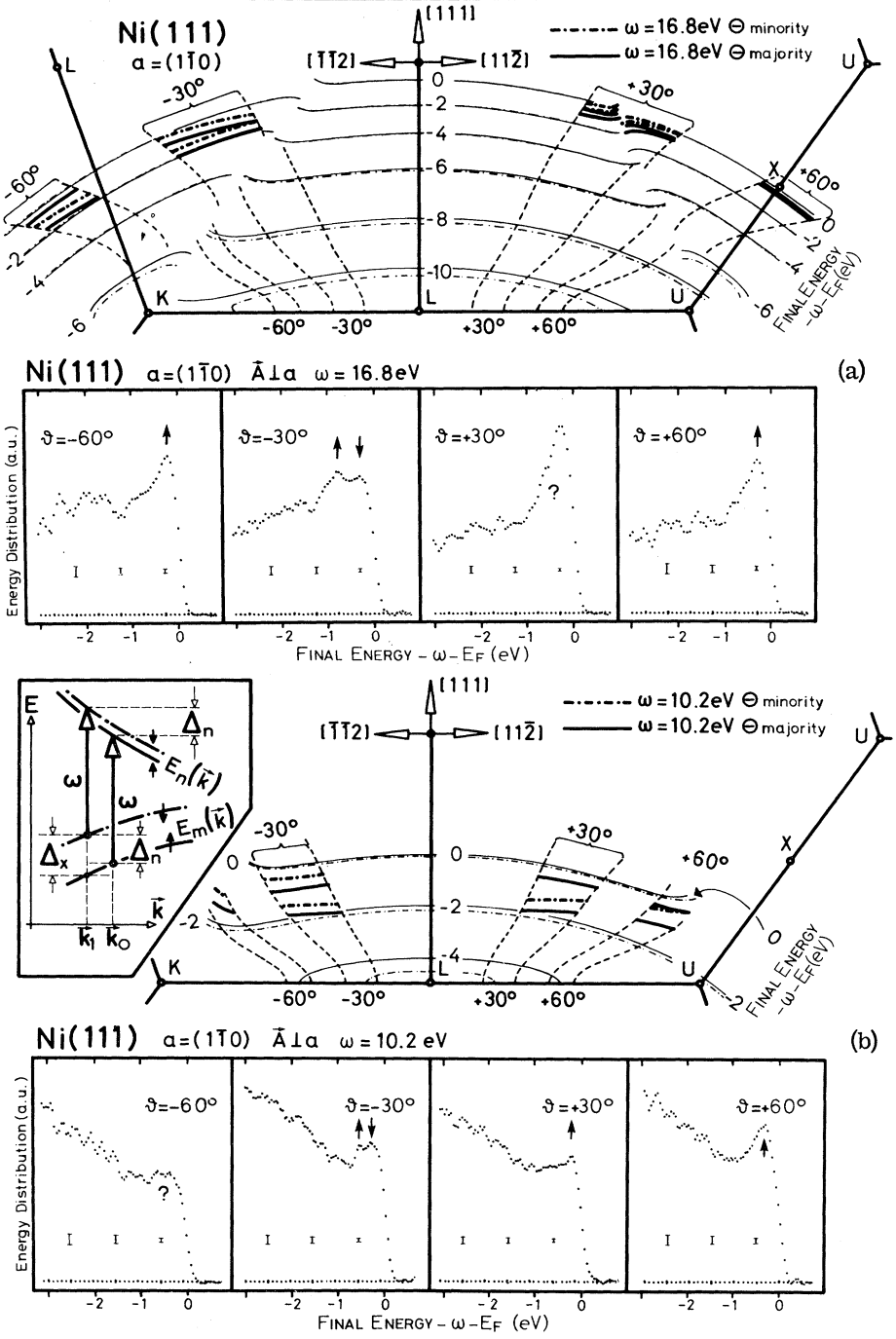

FIG. 1. (a) and (b) refer to the photon energy $\hbar\omega$ = 16.8 and 10.2 eV, respectively. The four energy distribution curves in each portion are obtained from a (111) surface for normal incidence of the plane-polarized radiation. The plane of polarization is perpendicular to the plane of detection in this plane are specified by the polar angle of emission ϑ. The negative and positive signs of ϑ refer to the component $\vec{\kappa}$ of the wave vector in vacuum being parallel to [$\bar{1}\bar{1}$2] and [11$\bar{2}$], respectively. Also shown is the corresponding (1$\bar{1}$0) plane of the Brillouin zone. The light and heavy lines are lines of constant final energy and the optical lines of constant energy difference, respectively, with the solid and dash-dotted lines corresponding to the majority- and minotiry-spin states. The dashed lines are the lines of momentum conservation $\vec{k}_t = \vec{\kappa}$ in the emission for constant ϑ. The arrows in the spectra denote transitions between majority- and minority-spin states, while the question marks refer to the "gap" transitions discussed in the text.

for the minority-spin states, depending on the region of $\vec{k}$ space investigated. We therefore concentrate on this component in the following.

The doublet observed for both photon energies at $\vartheta = -30°$, centered at about -0.5 eV, clearly arises from the higher-energy minority- and majority-spin components, since the minority-spin states are occupied here. On the other hand, the top minority-spin states are empty for $\hbar\omega = 16.8$ eV, $\vartheta = \pm 60°$ and for $\hbar\omega = 10.2$ eV, $\vartheta = +30°$ and $+60°$, explaining the single peak observed there. The lines of constant final energy show "gaps" for $\hbar\omega = 16.8$ eV near the $\vartheta = +30°$ region and for $\omega = 10.2$ eV near $\vartheta = -60°$. The final states are no longer dominated by one plane-wave component near these gaps, i.e., they mark the transition between zeroth-order and surface umklapp emission, or, in the terminology of Mahan,[13] between primary and secondary cones. Since secondary-cone emission tends to the weak,[8] we do not attempt a detailed analysis in these cases. The lower-energy odd-parity component of the initial states might be responsible for some of the structure observed at lower energies. However, we do not attempt a definite assignment, since this structure is weaker and the statistical error larger than for the higher-energy structure.

The doublet splitting Δ_n observed for $\vartheta = -30°$ is not identical to the exchange splitting Δ_x, as is apparent from the inset in Fig. 1(b). They are connected by the equation

$$\Delta_n = E_n^{\uparrow}(\vec{k}_1) - E_n^{\uparrow}(\vec{k}_0) = E_m^{\uparrow}(\vec{k}_1) - E_m^{\uparrow}(\vec{k}_0) + \Delta_x. \quad (2)$$

The experimental and theoretical numbers for Δ_x are compared in Table I. As seen from this table, the exchange splitting calculated by Wang and Callaway[1] using the vBH exchange-correlation potential agrees much better with the experimental values than the corresponding value for the Kohn-Sham-Gaspar (KSG) exchange potential.[14] The vBH energy bands of Wang and Callaway also happen to give a much better agreement with the measured magneton number.[1] The vBH value for Δ_x is still about 0.15 eV higher than the Δ_x determined from our experiment. We should remark here that the value for Δ_x measured for $\hbar\omega = 16.8$ eV is probably more reliable than the corresponding value for $\hbar\omega = 10.2$ eV where the difference between Δ_n and Δ_x is relatively large.

In spite of these numerical deviations, the overall agreement between the vBH energy bands of Wang and Callaway and the experiments is quite good, in particular with respect to the appearence and disappearence of the doublet structure. We emphasize again that the identification of this structure is possible only with the help of the optical selection rule, which is the important feature of our experiment. The spectra corresponding to the ones given in Fig. 1 but with the plane of polarization parallel to $(1\bar{1}0)$ do not show any pronounced structure near E_F. Our results, together with the apparent lack of strong temperature effects in the photoemission spectra when going through the transition temperature,[4,6] strongly support the "local band theory" model[15] which provides also the basis for the recent interpretation[16] of the new electron spin polarization measurements.[17]

TABLE I. Values of Δ_n and of the exchange splitting Δ_x.

ω (eV)	$\Delta_n^{\text{expt.}}$ (eV)	$\Delta_x^{\text{expt.}}$ (eV)	Δ_x^{vBH} [a] (eV)	Δ_x^{KSG} [b] (eV)
16.8	0.51	0.49 ± 0.05	0.60	0.84
10.2	0.30	0.35 ± 0.10	0.60	0.84

[a] Refs. 1 and 11. [b] Refs. 1 and 14.

We wish to thank C. S. Wang and J. Callaway for sending the high-energy $E(\vec{k})$ values which we fitted by the combined interpolation scheme. We are also grateful to L.-G. Petersson and R. Erlandsson for supplying us with their results prior to publication, to H. Becker, L. L. Hirst, and R. J. Jelitto for helpful discussions, and to G. Bender for growing the Ni crystal. This work is a project of the Sonderforschungsberich 65 "Festkörperspektroskopie."

[1] C. S. Wang, and J. Callaway, Phys. Rev. B 15, 298 (1977).
[2] M. Shiga and G. P. Pells, J. Phys. C 2, 1847 (1969).
[3] J. E. Rowe and J. C. Tracy, Phys. Rev. Lett. 27, 799 (1971).
[4] D. T. Pierce and W. E. Spicer, Phys. Rev. B 6, 1787 (1972).
[5] P. Heimann and H. Neddermeyer, J. Phys. F 6, L257 (1976).
[6] L.-G. Petersson and R. Erlandsson, in Proceedings of the Fifth International Conference on Vacuum Ultraviolet Radiation Physics, Montpellier, France, September 1977 (to be published).
[7] E. O. Kane, Phys. Rev. Lett. 12, 97 (1964).
[8] E. Dietz, H. Becker, and U. Gerhardt, Phys. Rev. Lett. 36, 1397 (1976), and 37, 115 (1976).

[9]H. Becker, E. Dietz, U. Gerhardt, and H. Angermüller, Phys. Rev. B 12, 2084 (1975).
[10]N. V. Smith and L. F. Mattheiss, Phys. Rev. B 9, 1341 (1974).
[11]U. von Barth and L. Hedin, J. Phys. C 5, 1629 (1972).
[12]J. Hermanson, Solid State Commun. 22, 9 (1977).
[13]G. D. Mahan, Phys. Rev. B 2, 4334 (1970).
[14]W. Kohn and L. J. Sham, Phys. Rev. 140, A1133 (1965); R. Gaspar, Acta Phys. Acad. Sci. Hung. 3, 263 (1954).
[15]V. Korenman, J. L. Murray, and R. E. Prange, Phys. Rev. B 16, 4032 (1977).
[16]D. G. Dempsey and Leonard Kleinman, Phys. Rev. Lett. 39, 1297 (1977).
[17]W. Eib and S. F. Alvarado, Phys. Rev. Lett. 37, 444 (1976).

Quantum Beats of Recoil-Free γ Radiation

Gilbert J. Perlow
Argonne National Laboratory, Argonne, Illinois 60439
(Received 9 February 1978)

Recoil-free γ rays from the decay of ^{57}Co are frequency modulated by vibrating the source with a piezoelectric crystal and one of the lines of the resulting multiplet emission spectrum is absorbed. The remaining radiation displays a time-dependent counting rate whose harmonic composition and relative phases are sensitive to small energy shifts and can be used for their measurement.

When a γ-ray emitter is vibrated sinusoidally with amplitude x_0 along the direction of observation, and with angular frequency Ω, the time dependence of the radiation field can be expressed as

$$E(t,t_0)=\begin{cases}\exp[-\lambda(t-t_0)/2+i(\omega_0 t+a\sin\Omega t)], & t\geq t_0,\\ 0, & t<t_0,\end{cases} \quad (1)$$

where λ^{-1} is the mean lifetime of the excited nuclear state (the lower state is assumed to be stable). The quantity $a\equiv\omega_0 x_0/c$ is called the modulation index. The origin of time has been chosen as a zero of the sine, and the decaying state was formed at $t=t_0$. Irrelevant normalization and phase factors have been omitted. In what follows, t_0 is never measured and must be averaged over. If one forms the average, $\langle|E(t,t_0)|^2\rangle_{t_0}$, the variable t disappears, so that, as expected, there is no time dependence of the intensity. The spectrum corresponding to Eq. (1) is obtained by squaring its Fourier transform and averaging over t_0. It is the familiar sum of Lorentzian-shaped carrier and sidebands, first shown with Mössbauer radiation by Ruby and Bolef[1] and observed and discussed by others since.[2-6]

$$I(\omega)=\sum_{n=-\infty}^{\infty} J_n^2(a)/\{[\omega-(\omega_0+n\Omega)]^2+\lambda^2/4\}, \quad (2)$$

where the J_n are Bessel functions of the first kind.

If we now interpose a resonant absorber between the vibrating source and the γ-ray detector, so that there are alterations in phase or amplitude among the components, a time dependence appears in the intensity. It contains the frequency Ω and its harmonics.

In Fig. 1(a), we see the ordinary Mössbauer velocity spectrum of a source of ^{57}Co diffused into a 12-μm foil of Cu which is cemented to one face of a 0.5 mm×9 mm diameter X-cut quartz crystal. The opposite face is cemented to an aluminum backing. The spectrum is made by scanning with a (slowly) moving absorber of ^{57}Fe-enriched sodium ferrocyanide. There is no voltage across the piezoelectric crystal. In Fig. 1(b), an rf generator has supplied 10 V at 9.95 MHz to the crystal and one sees the carrier and sideband pattern described by Eq. (2). In Fig. 1(c), the central carrier has been nearly eliminated by interposing a thick stationary absorber of ^{57}Fe in Be just after the source. Fe-Be has a broad resonance, actually an unresolved doublet, whose centroid corresponds closely to the energy of the ^{57}Co-Cu emission line. The ferrocyanide analyzing absorber is now removed and the radiation responsible for Fig. 1(c) is counted with a thin NaI scintillation counter in a fast timing circuit.